Biochemical and Biophysical Research Communications 425 (2012) 219–224

Contents lists available at SciVerse ScienceDirect

Biochemical and Biophysical Research Communications

journal homepage: www.elsevier.com/locate/ybbrc

The N-terminus of TDP-43 promotes its oligomerization and enhances DNA binding affinity

Chung-ke Chang [a,1], Tzong-Huah Wu [b,c,d,1], Chu-Ya Wu [b,e], Ming-hui Chiang [a], Elsie Khai-Woon Toh [a], Yin-Chih Hsu [b], Ku-Feng Lin [b], Yu-heng Liao [a], Tai-huang Huang [a,f,*], Joseph Jen-Tse Huang [b,*]

[a] Institute of Biomedical Sciences, Academia Sinica, Taipei 115, Taiwan
[b] Institute of Chemistry, Academia Sinica, Taipei 115, Taiwan
[c] Chemical Biology and Molecular Biophysics Program, Taiwan International Graduate Program, Institute of Biochemistry, Academia Sinica, Taipei 115, Taiwan
[d] Institute of Bioinformatics and Structural Biology, National Tsing Hua University, Hsinchu 300, Taiwan
[e] Graduate Institute of Engineering, National Taiwan University of Science and Technology, Taipei 106, Taiwan
[f] Department of Physics, National Taiwan Normal University, Taipei 106, Taiwan

ARTICLE INFO

Article history:
Received 9 July 2012
Available online 23 July 2012

Keywords:
TDP-43
DNA/RNA binding
Oligomerization
Neurodegenerative disease
N-terminus

ABSTRACT

TDP-43 is a DNA/RNA-binding protein associated with different neurodegenerative diseases such as amyotrophic lateral sclerosis (ALS) and frontotemporal lobar degeneration (FTLD-U). Here, the structural and physical properties of the N-terminus on TDP-43 have been carefully characterized through a combination of nuclear magnetic resonance (NMR), circular dichroism (CD) and fluorescence anisotropy studies. We demonstrate for the first time the importance of the N-terminus in promoting TDP-43 oligomerization and enhancing its DNA-binding affinity. An unidentified structural domain in the N-terminus is also disclosed. Our findings provide insights into the N-terminal domain function of TDP-43.

1. Introduction

TAR DNA binding protein (TDP-43) is a ubiquitously expressed DNA/RNA-binding protein implicated in gene transcription, pre-mRNA splicing and translational regulation [1,2]. It represses transcription in HIV-1 and causes exon skipping of the cystic fibrosis transmembrane regulator (CFTR) gene [3,4]. TDP-43 contains two RNA recognition motifs (RRMs), RRM1 and RRM2, which primarily recognize single-stranded $(TG)_n/(UG)_n$ repeats, although recognition of other pyrimidine-rich sequences at lower affinity has also been reported [2,5,6]. The C-terminus of TDP-43 is an intrinsically disordered region which interacts with heterogeneous nuclear ribonucleoprotein (hnRNP) A2 and fused-in-sarcoma/translated-in-liposarcoma (FUS/TLD), and might be involved in RNA processing [7,8].

Recently, TDP-43 has also been shown to be the major component associated with two important neurodegenerative diseases including amyotrophic lateral sclerosis (ALS), a common motor neuron disease, and frontotemporal lobar degeneration with ubiquitin inclusions (FTLD-U), the second-most common dementia afflicting humans [4]. In the neuronal inclusions of these patients, N-terminally truncated TDP-43 could be easily found. These findings implied TDP-43 as a major culprit in neuropathology, a subset now known as TDP-43 proteinopathies. While the C-terminus has been shown to be the major region associated with ALS/FTLD-U due to its ability to form aggregates [9–12] and amyloid fibers *in vitro* [13], other studies have also suggested that the DNA/RNA binding activity of TDP-43 could play a role in these diseases [6,14,15].

In contrast, the biochemical and pathological roles of the N-terminus have been seldom studied. Research in yeast and mammalian cells have shown that the loss of the N-terminus may enhance aggregation, thus underscoring its potential importance in TDP-43 function and possible roles in pathogenesis [16,17]. Here, we have characterized the structural and physical properties of the N-terminus of TDP-43. Our results indicate that the N-terminus contains an unidentified structural domain and promotes oligomerization in a concentration-dependent fashion. Moreover, the presence of the N-terminus enhances the binding of the two RRM domains towards single-stranded $(TG)_6$ DNA. The consequences of our findings are discussed in the context of TDP-43 function.

* Corresponding authors. Addresses: Institute of Biomedical Sciences, Academia Sinica, Taipei 115, Taiwan (T.-h. Huang), Institute of Chemistry, Academia Sinica, Taipei 115, Taiwan (J.J.-T. Huang). Fax: +886 2 2788 7641 (T.-h. Huang), +886 2 2783 1237 (J.J.-T. Huang).
E-mail addresses: bmthh@gate.sinica.edu.tw (T.-h. Huang), jthuang@chem.sinica.edu.tw (J.J.-T. Huang).
[1] These authors contributed equally to this study.

0006-291X/$ - see front matter © 2012 Elsevier Inc. All rights reserved.
http://dx.doi.org/10.1016/j.bbrc.2012.07.071

2. Material and methods

2.1. Plasmid construction

TDP_{1-105}, $TDP_{106-265}$ and TDP_{1-265} were subcloned from vector containing full-length TDP-43 (a generous gift from Dr. Benjamin Tu, Academia Sinica) into pET-17b plasmid (Novagen, MA) with sequences encoding a short His_6-tag inserted at the N-terminus of the protein for purification purposes. pQE-30 (Qiagen, CA) vectors encoding $TDP_{101-191}$, $TDP_{192-265}$, or $TDP_{101-265}$ with a N-terminal His_6-tag was a kind gift from Dr. Hanna Yuan (Academia Sinica).

2.2. Protein expression and purification

Different experimental conditions were applied to obtain proper expression and purification of the truncated TDP protein (details in Supplemental Materials). Truncated TDP proteins were expressed in *Escherichia coli* BL21 (de3) or M15 strains in LB media and the cells lysed by French press or microfluidizer. The lysate was centrifuged at 15,000*g* for 1 h. His-tagged proteins were purified by passing the soluble lysate through Ni^{2+}-chelated resin and washed/eluted with buffer containing 20–400 mM imidazole. Eluted proteins were subjected to further purification with a size exclusion column. The purified protein was confirmed by sodium dodecyl sulfate polyacrylamide gel electrophoresis (SDS–PAGE) with the NuPage SDS–PAGE system (Invitrogen, CA). Isotope-labeled protein samples were prepared by culturing the cells in M9 media supplemented with $^{15}NH_4Cl$ (Isotec, OH) and, in the case of deuterated samples, D_2O. Protein concentrations were determined by measuring the optical absorbance at 280 nm with a Beckman DU-800 (Beckman Coulter, IN) or Nanodrop ND-1000 (Thermo Scientific, MA) spectrophotometer.

2.3. Nuclear magnetic resonance (NMR) spectroscopy

Proteins were dissolved in buffer (25 mM HEPES, 150 mM NaCl, 1 mM DTT, 10% D_2O, pH 6.3 or 7.4) for NMR experiments. Protein concentration and buffer pH were chosen on the basis of protein stability/solubility. Spectra were acquired at 25 °C on a Bruker Avance III 600-MHz spectrometer equipped with a TCI cryoprobe. Data were processed with TopSpin 3.0 (Bruker, Germany) and iNMR (Nucleomatica, Italy). The ^1H chemical shift was referenced to 2,2-dimethyl-2-silapentane-5-sulfonate (DSS) at 0 ppm and the ^{15}N chemical shift was referenced indirectly according to the IUPAC recommendations [18].

2.4. Circular dichroism (CD) spectroscopy

CD measurements were performed on 5 μM protein with a Jasco J-815 spectropolarimeter (Jasco, Tokyo, Japan) by scanning the wavelength from 260 nm to 190 nm at 25 °C. A cuvette with a pathlength of 1 mm was used. The secondary structure content was estimated on the DICHROWEB server with the CDSSTR algorithm using Reference Set #7, which contains a mix of structured and disordered proteins, as the reference database [19,20].

2.5. Analytical size-exclusion chromatography (SEC)

All SEC experiments were performed on AKTA fast protein liquid chromatography (FPLC) systems at 4 °C with the elution profiles monitored through absorbance at 280 nm. Protein in running buffer (25 mM HEPES, 150 mM NaCl, 1 mM DTT, 50 mM arginine, 50 mM glutamic acid, pH 7.4) was passed through a Superdex-75/60 HiLoad column (GE Healthcare, MA) pre-calibrated with the Gel Filtration LMW Calibration Kit (GE Healthcare, MA) with a flow rate of 1 mL/min. Lower concentration samples were prepared by directly diluting the higher concentration samples with running buffer.

2.6. Fluorescence anisotropy

Fluorescence anisotropy measurements were acquired on a Chronos-FD spectrofluorimeter (ISS, IL) with an excitation and emission wavelength of 473 and 536 nm, respectively. Single-stranded $(TG)_6$ DNA with 6-carboxyfluorescein (FAM) at its 5′-end was purchased (Protech Systems, Taiwan). Binding reactions were carried out in reaction buffer (10 mM sodium phosphate and 1 mM EDTA, pH 8.0) with a final DNA concentration of 10 nM. Anisotropy values were calculated from the fluorescence intensity (I) and gain (G) in parallel and perpendicular modes using the relation $R = (R_V - R_H)/(R_V + 2R_H)$, where $R_H = G_{\|}I_{\|}/G_{\perp}I_{\perp}$ and $R_V = G_{\|}/G_{\perp}$ [21,22]. Binding constants were obtained by analyzing the data with GraphPad Prism 5 software (GraphPad, CA).

3. Results

3.1. Structural features and domain arrangement of the NTD in TDP-43

The Regional Order Neural Network (RONN) protein order–disorder predictor was applied to predict the conformation within

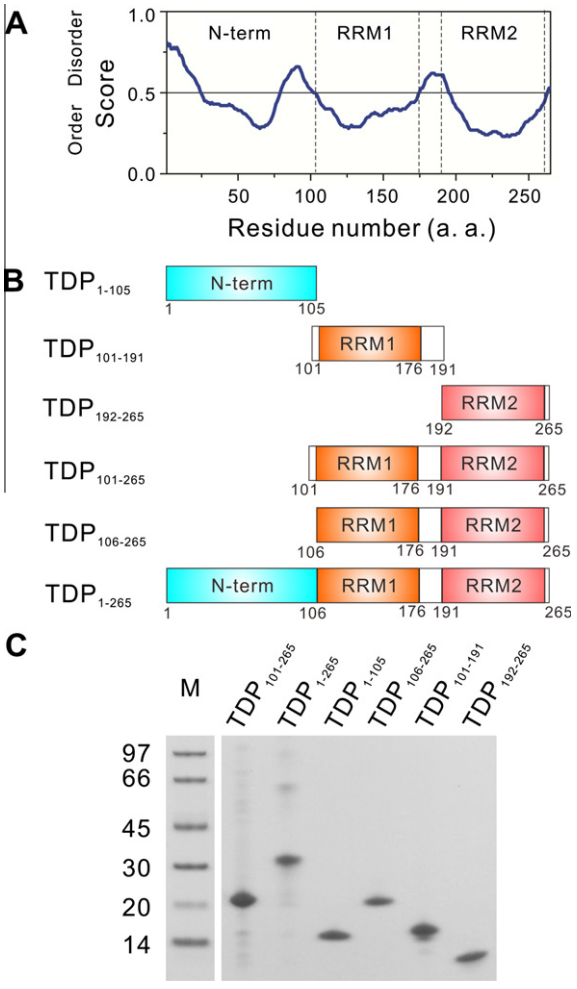

Fig. 1. (A) Order/disorder region of TDP_{1-265} predicted by DisEMBL. (B) Schematic of different TDP constructs used in this study. (C) SDS–PAGE of purified proteins including $TDP_{101-265}$, TDP_{1-265}, TDP_{1-105}, $TDP_{106-265}$, $TDP_{101-191}$ and $TDP_{192-265}$.

TDP_{1-265} and suggested an ordered region within its N-terminus (Fig. 1A) [23]. This prediction is consistent with recent literature, but has never been confirmed experimentally [13]. We constructed various TDP-43 truncations (Fig. 1B) and characterized their purities (⩾95%) by SDS–PAGE (Fig. 1C). ^{15}N-edited heteronuclear single-quantum coherence spectra (^{15}N-HSQC) have been widely used as a tool to monitor order/disorder in proteins [24]. For large proteins, ^{15}N-HSQC often suffers from low sensitivity due to fast transverse relaxation effects and it is essential to obtain ^{15}N-TROSY (^{15}N-edited transverse relaxation optimized spectroscopy) of perdeuterated and uniformly ^{15}N-labeled protein samples for structural characterization [25]. In the case of TDP_{1-105}, it was necessary to use extremely low concentrations (~20 μM) of perdeuterated protein to obtain quality ^{15}N-TROSY spectrum (Fig. 2A) due to its aggregation-prone potency, suggesting that even at this low concentration TDP_{1-105} is not in a pure monomeric state. Nonetheless, the resonance dispersion on the ^{1}H axis suggested the presence of a structural domain within this construct. Clustering of resonances between 7.5–8.5 ppm on the ^{1}H axis also identified the possible existence of helices or disordered regions in TDP_{1-105}. The presence of helix in TDP_{1-105} can be ruled out from CD analysis as discussed below. The structures of RRM1 ($TDP_{101-191}$) and RRM2 ($TDP_{192-265}$) have been solved and their ^{15}N-HSQC spectra are well dispersed, as expected (Fig. 2B) [26,27]. The ^{15}N-HSQC spectrum of TDP_{1-265} is composed of many well-resolved resonances and some resonances clustered around 7.5–8.5 ppm in the proton dimension (blue resonances on Fig. 2C). When overlaid on the ^{15}N-HSQC of TDP_{1-105} (red resonances on Fig. 2C), the two spectra showed a number of well-superimposed dispersed resonances, indicating that the structural domain at the N-terminus is preserved in TDP_{1-265}. The ^{15}N-HSQC spectrum $TDP_{101-265}$, the di-domain consisting of RRM1 and RRM2, is practically the sum of the ^{15}N-HSQC spectra of RRM1 and RRM2, suggesting that the two RRMs are independent structural entities with little interaction between them (magenta resonances on Fig. 2B). To investigate whether the structure of the two RRMs were perturbed by the presence of the N-terminal domain (NTD), we have superimposed the spectrum of $TDP_{101-265}$ onto that of TDP_{1-265} (Fig. 2D). Interestingly, the resonance positions between the spectra of the two constructs were quite matched, which hinted that the structures of the two RRM domains are not perturbed by linking them to the N-terminus between the NTD and the two RRMs in TDP-43.

The low concentration necessary to obtain quality spectrum for TDP_{1-105} precluded our ability to assign the resonances and solve the structure of the NTD. To obtain more information about the structure, we compared the CD spectra of TDP_{1-105}, $mTDP_{106-265}$ and TDP_{1-265} (Fig. 2E). Their secondary structure contents were estimated through decomposition analysis of CD spectra and listed in Table 1. The results for $TDP_{106-265}$ is in good agreement with that calculated from the determined structures of RRM1 and RRM2. Different from other domains, TDP_{1-105} showed preponderance towards β-strand (~35%) and unordered structures (~45%) that were consistent with secondary structure predictions (results not shown). This result was also consistent with the NMR spectral features of TDP_{1-105} (Fig. 2A), namely the generally well-dispersed resonance pattern – often a hallmark of proteins containing β-sheet structure – and the cluster of resonances between 7.5–8.5 ppm on the ^{1}H axis representing disordered structure.

3.2. Oligomerization properties of the NTD

To obtain insights into the possible function of the NTD, analytical SEC was used to characterize the biophysical properties of different TDP-43 fragments (Fig. 3A–C). We observed a gradual shift in the retention volume of the main peak of TDP_{1-105} (Fig. 3A) with concentration, which was recapitulated by the same experiments with TDP_{1-265} (Fig. 3C). On the other hand, $TDP_{106-265}$ eluted out with the same retention volume at 20 and 100 μM protein concentrations (Fig. 3B). It is noted that $TDP_{106-265}$ aggregation increased dramatically at concentrations above 150 μM, thus preventing us from further SEC analysis. Since the low-concentration samples were obtained by directly diluting the high-concentration samples with buffer, our results suggested that TDP_{1-105} is capable of

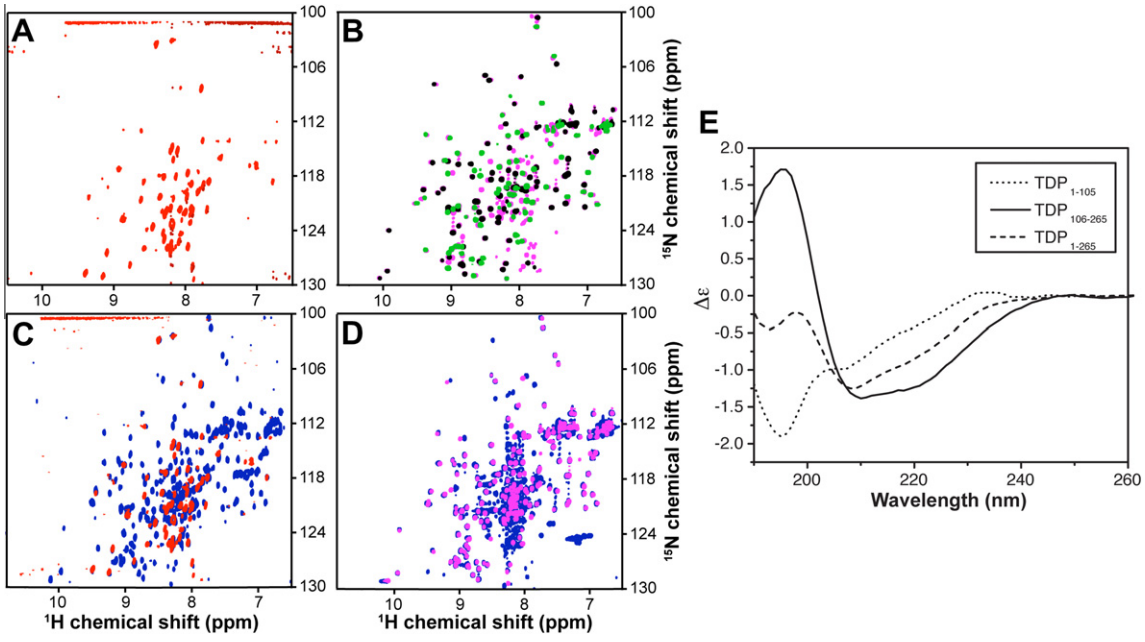

Fig. 2. NMR and CD spectra of TDP-43 constructs. (A) ^{15}N-TROSY spectrum of 20 μM TDP_{1-105} at pH 6.3. (B) ^{15}N-HSQC spectra overlay of 200 μM $TDP_{101-191}$ (black), 200 μM $TDP_{192-265}$ (green), and 100 μM $TDP_{101-265}$ (magenta) at pH 7.4. (C) Overlay of 20 μM TDP_{1-265} ^{15}N-HSQC (blue) and 20 μM TDP_{1-105} ^{15}N-TROSY (red) spectra at pH 6.3. The TROSY spectrum has been shifted to match the chemical shift referencing of the HSQC spectrum. (D) Spectrum overlay of 100 μM $TDP_{101-265}$ (magenta) and 20 μM TDP_{1-265} (blue) at pH 7.4. (E) CD spectra of TDP_{1-105} (dotted line), $TDP_{106-265}$ (solid line), and TDP_{1-265} (dashed line).

Table 1
Predicted secondary structure composition from the CD analysis of TDP-43 variants.

Construct	Helix (%)	Strand (%)	Turn (%)	Unordered (%)
TDP_{1-105}	1	34	18	44
$TDP_{106-265}$	18	27	20	35
TDP_{1-265}	3	35	20	39

oligomerization in a dynamic and reversible manner. At higher concentrations, additional peaks eluted out before the main peak in the chromatograms for both TDP_{1-105} and TDP_{1-265}, indicating the presence of other larger oligomer species. Our results showed that more than one oligomer species are present in solution whenever the NTD is included in the construct, indicating that the NTD promotes reversible oligomerization of TDP-43.

Additional evidence is provided by the concentration dependence of the NTD NMR spectra (Fig. 3D–G). The line widths of resonances are more uniform at 20 μM TDP_{1-105} concentration (Fig. 3D) than at 400 μM concentration (Fig. 3E). Increasing TDP_{1-105} concentration resulted in a gradual decrease in intensity of the well-dispersed resonances (Fig. 3F), whereas resonances between 7.5–8.5 ppm on the ^{1}H axis remained largely the same (Fig. 3G). At protein concentrations above ~100 μM, the well-dispersed resonances broaden out even when using perdeuterated protein and TROSY experiments (Supplemental Fig. S2), suggesting that large oligomers are formed at higher concentrations that are beyond the size limit of current NMR technique. It is noted that while the NMR and SEC results are in qualitative agreement, the effective concentrations in the SEC column is much less than those in the NMR tube because of the column dilution factor during the chromatography run, resulting in much larger oligomers at a given concentration for the NMR experiments. The fact that the resonances between 7.5–8.5 ppm on the ^{1}H axis retain their signal at higher protein concentrations indicated that the resonances arising from flexible regions within TDP_{1-105} remain flexible when large oligomers are formed and implied that the contact residues during the oligomerization process reside in the structured region of the NTD.

3.3. The NTD contributes towards nucleic acid binding of TDP-43

Both RRM1 and RRM2 have been reported to bind strongly to either single-stranded or double-stranded DNA/RNA [2]. In an attempt to confirm whether the presence of NTD may affect other biochemical properties of TDP-43, we conducted fluorescence anisotropy measurements to monitor the binding of different TDP-43 fragments towards single-stranded DNA (Fig. 4), $ss(TG)_6$, and analyzed their binding properties (Table 2). We found that TDP_{1-105} did not bind to $ss(TG)_6$ significantly (Fig. 4A), but

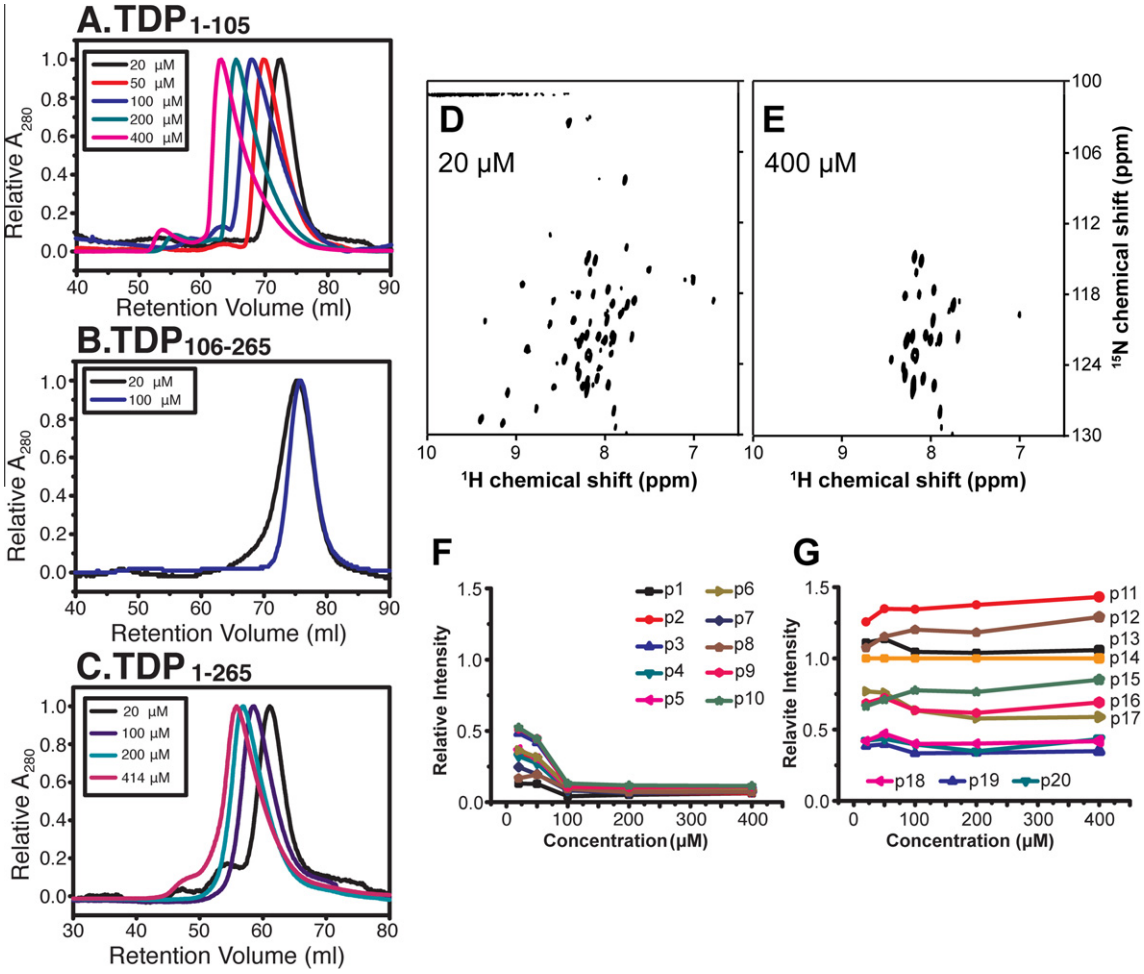

Fig. 3. Effect of protein concentration on oligomerization of NTD. Analytical gel filtration results at different protein concentrations are shown for (A)TDP_{1-105}, (B)$TDP_{106-265}$, and (C)TDP_{1-265}. Absorptions at 280 nm were normalized to the highest peak of each chromatogram. Raw data chromatograms are shown in Supplemental Fig. S1. ^{15}N-TROSY spectra of TDP_{1-105} at (D) 20 μM and (E) 400 μM are also shown. Relationship between peak intensity and protein concentration for selected resonances are shown in (F) for well-dispersed resonances and (G) for resonances clustered between 7.5–8.5 ppm on the ^{1}H dimension. All peak intensities were normalized to that of peak *p14* at 20 μM protein concentration. Resonance positions are listed in Supplemental Table S1 and spectra at 50, 100 and 200 μM are shown in Supplemental Fig. S2.

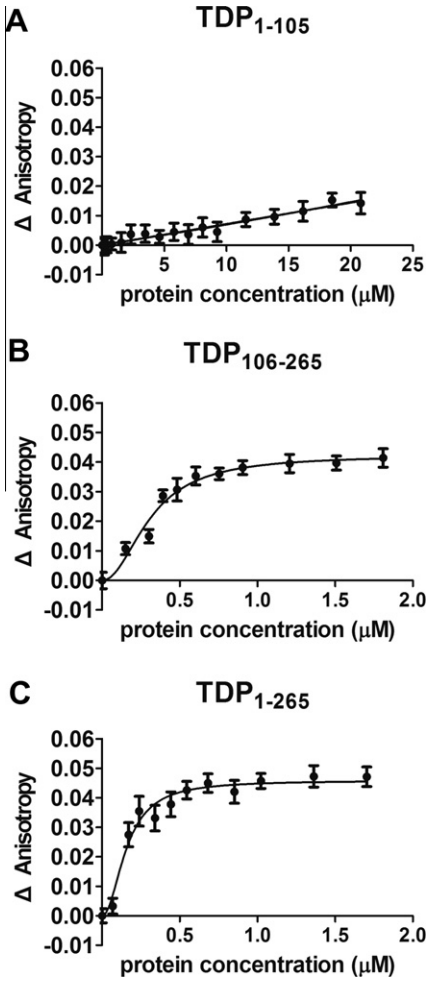

Fig. 4. Binding isotherms of TDP variants to ssDNA monitored by fluorescence anisotropy spectroscopy. The anisotropy changes in fluorophore-attached $ss(TG)_6$ upon binding to TDP_{1-105}, $TDP_{106-265}$, and TDP_{1-265} are shown in (A)–(C), respectively.

Table 2
The DNA binding parameters of TDP-43 derived from the fluorescence anisotropy studies.

	TDP_{1-105}	$TDP_{106-265}$	TDP_{1-265}
Kd (nM)	$>4 \times 10^{7}$[a]	312 ± 12	100 ± 6
n_H	N. A.[a]	2.1 ± 0.2	1.8 ± 0.2

[a] Non-specific binding.

TDP_{1-265} showed a 3-fold increase in apparent binding affinity compared to $TDP_{106-265}$ (Fig. 4B and C). The Hill coefficients (n_H) for TDP_{1-265} and $TDP_{106-265}$ were both close to 2, which suggested that each oligonucleotide bound more than one polypeptide chain. Based on these results and our findings regarding the oligomerization properties of the NTD discussed above, we suggest that the additional binding energy originated from the NTD–NTD interactions.

4. Discussion

It is evident that the three structural domains (NTD, RRM1 and RRM2) of TDP-43 are arranged in a "beads on a string" fashion with each domain acting as an independently folded entity (Fig. 2). The NTD acts as an oligomerization domain in a concentration dependent manner, and NTD–NTD interactions most likely require the structured region. Our CD data lead us to surmise that the structured region of the NTD should be rich in β-strands (Fig. 2E), so the oligomerization is probably mediated by a β-sheet structure. At first glance, structural studies of the NTD should be amenable to a "divide-and-conquer" approach; however, structure determination of the NTD is hampered by its intrinsic properties: the extremely low concentration required to obtain good NMR spectra makes solution structure determination unfeasible whereas high intrinsic disorder content (Fig. 1 and Table 1) and dynamic oligomerization behavior will pose problems during crystallization [28].

It has been previously reported that the dimerization of TDP-43 *in vivo* required the presence of both the NTD and RRM1 with neither alone being sufficient for promoting dimerization, whereas our SEC results suggest that the NTD alone is capable of oligomer formation (Fig. 3) [29,30]. This discrepancy may arise from the different methodologies employed in these experiments. While the former utilized non-equilibrium pull-down methods that tend to underestimate the amount of oligomers in dynamic equilibrium due to extensive washing of the binding matrix [31], the latter did not require a washing step and was able to preserve the weak NTD–NTD interaction. Further stabilization of the TDP-43 dimer *in vivo* could be provided by RRM1 in the form of ternary interactions such as binding to RNA or self-association in addition to the NTD–NTD interaction [2].

There is still little information on the functional role of the NTD, making it difficult to speculate how NTD oligomerization could impact TDP-43 function. One possibility is for NTD oligomers to form an interaction platform for other proteins such as nuclear factor κB (NF-κB), which was reported to interact with the NTD and probably involved in microglia-mediated neurotoxicity [32]. A second possibility based on our findings (Fig. 4) is for NTD oligomers to act as a facilitator of TDP-43 nucleic acid binding. While $ss(TG)_6$ has an average of 1–2 protein-binding sites, thus limiting the number of possible protein–protein interactions, longer nucleotide sequences would be able to bind to a larger number of proteins and lead to increased NTD–NTD interaction [33]. Furthermore, nonspecific interactions between TDP-43 and DNA/RNA could elevate the local concentration of the NTD at the binding sites, resulting in enhanced NTD–NTD interaction [2]. The additional free energy from these interactions could help TDP-43 bind to lower affinity but functionally important sites such as the 3′-untranslated region of its own transcript and sparse UG-rich sequences [6,14]. However, whether such a coupling between nucleic acid binding activity and oligomerization of TDP-43 really exists and how it would work remains to be determined.

In summary, we established the structural domain arrangement of the NTD, RRM1 and RRM2 in TDP-43 and carried out biophysical characterization of the NTD. The NTD is involved in homotypic interactions and likely modulates nucleic acid binding properties of TDP-43 in an indirect fashion. Considering the lack of understanding of the role NTD plays in TDP-43 function, our findings provide a basis for comprehensive studies on the functional and structural aspects of the NTD in the future.

Acknowledgments

This work was supported by research grants from Academia Sinica and The National Science Council of the Republic of China (Grants NSC 97-2113-M-001-003-MY2, 98-2113-M-001-015-MY2, and NSC 100-2113-M-001-013-MY2 to J.J.H.; NSC100-2321-B-001-028 and NSC100-2311-B-001-023 to T.H.H.). T.-H.Y. was supported by Academia Sinica. We would like to thank Dr. Benjamin Tu and Dr. Hanna Yuan from Academia Sinica for providing full-length TDP-43, $TDP_{101-191}$, $TDP_{192-265}$ and $TDP_{101-265}$ plasmids. We also thank the mass spectrometry support from Dr. Mei-Chun

Tseng and the suggestions of NMR experiments from Dr. Chi-fon Chang and Sunney I. Chan. NMR experiments were carried out with NMR spectrometers of the High-Field Nuclear Magnetic Resonance Center (HFNMRC) supported by National Research Program for Genomic Medicine, The National Science Council of the Republic of China.

Appendix A. Supplementary data

Supplementary data associated with this article can be found, in the online version, at http://dx.doi.org/10.1016/j.bbrc.2012.07.071.

References

[1] E. Buratti, F.E. Baralle, Multiple roles of TDP-43 in gene expression, splicing regulation, and human disease, Front. Biosci. 13 (2008) 867–878.
[2] P.H. Kuo, L.G. Doudeva, Y.T. Wang, C.K. Shen, H.S. Yuan, Structural insights into TDP-43 in nucleic-acid binding and domain interactions, Nucleic Acids Res. 37 (2009) 1799–1808.
[3] E. Buratti, A. Brindisi, F. Pagani, F.E. Baralle, Nuclear factor TDP-43 binds to the polymorphic TG repeats in CFTR intron 8 and causes skipping of exon 9: a functional link with disease penetrance, Am. J. Hum. Genet. 74 (2004) 1322–1325.
[4] M. Neumann, D.M. Sampathu, L.K. Kwong, A.C. Truax, M.C. Micsenyi, T.T. Chou, J. Bruce, T. Schuck, M. Grossman, C.M. Clark, L.F. McCluskey, B.L. Miller, E. Masliah, I.R. Mackenzie, H. Feldman, W. Feiden, H.A. Kretzschmar, J.Q. Trojanowski, V.M. Lee, Ubiquitinated TDP-43 in frontotemporal lobar degeneration and amyotrophic lateral sclerosis, Science 314 (2006) 130–133.
[5] S.H. Ou, F. Wu, D. Harrich, L.F. García-Martínez, R.B. Gaynor, Cloning and characterization of a novel cellular protein, TDP-43, that binds to human immunodeficiency virus type 1 TAR DNA sequence motifs, J. Virol. 69 (1995) 3584–3596.
[6] Y.M. Ayala, L. De Conti, S.E. Avendano-Vazquez, A. Dhir, M. Romano, A. D'Ambrogio, J. Tollervey, J. Ule, M. Baralle, E. Buratti, F.E. Baralle, TDP-43 regulates its mRNA levels through a negative feedback loop, EMBO J. 30 (2011) 277–288.
[7] A. D'Ambrogio, E. Buratti, C. Stuani, C. Guarnaccia, M. Romano, Y.M. Ayala, F.E. Baralle, Functional mapping of the interaction between TDP-43 and hnRNP A2 in vivo, Nucleic Acids Res. 37 (2009) 4116–4126.
[8] S.C. Ling, C.P. Albuquerque, J.S. Han, C. Lagier-Tourenne, S. Tokunaga, H. Zhou, D.W. Cleveland, ALS-associated mutations in TDP-43 increase its stability and promote TDP-43 complexes with FUS/TLS, Proc. Natl. Acad. Sci. USA 107 (2010) 13318–13323.
[9] B.S. Johnson, D. Snead, J.J. Lee, J.M. McCaffery, J. Shorter, A.D. Gitler, TDP-43 is intrinsically aggregation-prone, and amyotrophic lateral sclerosis-linked mutations accelerate aggregation and increase toxicity, J. Biol. Chem. 284 (2009) 20329–20339.
[10] M.A. Gitcho, R.H. Baloh, S. Chakraverty, K. Mayo, J.B. Norton, D. Levitch, K.J. Hatanpaa, C.L. White, E.H. Bigio, R. Caselli, M. Baker, M.T. Al-Lozi, J.C. Morris, A. Pestronk, R. Rademakers, A.M. Goate, N.J. Cairns, TDP-43 A315T mutation in familial motor neuron disease, Ann. Neurol. 63 (2008) 535–538.
[11] E. Kabashi, P.N. Valdmanis, P. Dion, D. Spiegelman, B.J. McConkey, C. Vande Velde, J.-P. Bouchard, L. Lacomblez, K. Pochigaeva, F. Salachas, P.-F. Pradat, W. Camu, V. Meininger, N. Dupre, G.A. Rouleau, TARDBP mutations in individuals with sporadic and familial amyotrophic lateral sclerosis, Nat. Genet. 40 (2008) 572–574.
[12] A. Yokoseki, A. Shiga, C.-F. Tan, A. Tagawa, H. Kaneko, A. Koyama, H. Eguchi, A. Tsujino, T. Ikeuchi, A. Kakita, K. Okamoto, M. Nishizawa, H. Takahashi, O. Onodera, TDP-43 mutation in familial amyotrophic lateral sclerosis, Ann. Neurol. 63 (2008) 538–542.
[13] A.K. Chen, R.Y. Lin, E.Z. Hsieh, P.H. Tu, R.P. Chen, T.Y. Liao, W. Chen, C.H. Wang, J.J. Huang, Induction of amyloid fibrils by the C-terminal fragments of TDP-43 in amyotrophic lateral sclerosis, J. Am. Chem. Soc. 132 (2010) 1186–1187.
[14] J.R. Tollervey, T. Curk, B. Rogelj, M. Briese, M. Cereda, M. Kayikci, J. Konig, T. Hortobagyi, A.L. Nishimura, V. Zupunski, R. Patani, S. Chandran, G. Rot, B. Zupan, C.E. Shaw, J. Ule, Characterizing the RNA targets and position-dependent splicing regulation by TDP-43, Nat. Neurosci. 14 (2011) 452–458.
[15] G.S. Pesiridis, K. Tripathy, S. Tanik, J.Q. Trojanowski, V.M. Lee, A "two-hit" hypothesis for inclusion formation by carboxyl-terminal fragments of TDP-43 protein linked to RNA depletion and impaired microtubule-dependent transport, J. Biol. Chem. 286 (2011) 18845–18855.
[16] H.Y. Li, P.A. Yeh, H.C. Chiu, C.Y. Tang, B.P. Tu, Hyperphosphorylation as a defense mechanism to reduce TDP-43 aggregation, PLoS One 6 (2011) e23075.
[17] B.S. Johnson, J.M. McCaffery, S. Lindquist, A.D. Gitler, A yeast TDP-43 proteinopathy model: exploring the molecular determinants of TDP-43 aggregation and cellular toxicity, Proc. Natl. Acad. Sci. USA 105 (2008) 6439–6444.
[18] J.L. Markley, A. Bax, Y. Arata, C.W. Hilbers, R. Kaptein, B.D. Sykes, P.E. Wright, K. Wuthrich, Recommendations for the presentation of NMR structures of proteins and nucleic acids. IUPAC–IUBMB–IUPAB inter-union task group on the standardization of data bases of protein and nucleic acid structures determined by NMR spectroscopy, J. Biomol. NMR 12 (1998) 1–23.
[19] N. Sreerama, R.W. Woody, Estimation of protein secondary structure from circular dichroism spectra: comparison of CONTIN, SELCON, and CDSSTR methods with an expanded reference set, Anal. Biochem. 287 (2000) 252–260.
[20] L. Whitmore, B.A. Wallace, DICHROWEB, an online server for protein secondary structure analyses from circular dichroism spectroscopic data, Nucleic Acids Res. 32 (2004) W668–673.
[21] J.R. Lakowicz, Principles of Fluorescence Spectroscopy, Plenum Press, New York, 1983.
[22] H.V. Patel, A.A. Vyas, K.A. Vyas, Y.S. Liu, C.M. Chiang, L.M. Chi, W. Wu, Heparin and heparan sulfate bind to snake cardiotoxin. Sulfated oligosaccharides as a potential target for cardiotoxin action, J. Biol. Chem. 272 (1997) 1484–1492.
[23] Z.R. Yang, R. Thomson, P. McNeil, R.M. Esnouf, RONN: the bio-basis function neural network technique applied to the detection of natively disordered regions in proteins, Bioinformatics 21 (2005) 3369–3376.
[24] P. Garcia, L. Serrano, M. Rico, M. Bruix, An NMR view of the folding process of a CheY mutant at the residue level, Structure 10 (2002) 1173–1185.
[25] K. Pervushin, R. Riek, G. Wider, K. Wuthrich, Attenuated T2 relaxation by mutual cancellation of dipole–dipole coupling and chemical shift anisotropy indicates an avenue to NMR structures of very large biological macromolecules in solution, Proc. Natl. Acad. Sci. USA 94 (1997) 12366–12371.
[26] S. Suzuki, Y. Muto, M. Inoue, T. Kigawa, T. Terada, M. Shirouzu, S. Yokoyama, Solution structure of the RNA binding domain of TAR DNA-binding protein-43. PDB ID: 2CQG.
[27] F. He, Y. Muto, M. Inoue, T. Kigawa, M. Shirouzu, T. Terada, S. Yokoyama, Solution structure of RRM domain in TAR DNA-binding protein-43. PDB ID: 1WF0.
[28] W.N. Price 2nd, Y. Chen, S.K. Handelman, H. Neely, P. Manor, R. Karlin, R. Nair, J. Liu, M. Baran, J. Everett, S.N. Tong, F. Forouhar, S.S. Swaminathan, T. Acton, R. Xiao, J.R. Luft, A. Lauricella, G.T. DeTitta, B. Rost, G.T. Montelione, J.F. Hunt, Understanding the physical properties that control protein crystallization by analysis of large-scale experimental data, Nat. Biotechnol. 27 (2009) 51–57.
[29] T. Nonaka, F. Kametani, T. Arai, H. Akiyama, M. Hasegawa, Truncation and pathogenic mutations facilitate the formation of intracellular aggregates of TDP-43, Hum. Mol. Genet. 18 (2009) 3353–3364.
[30] Y. Shiina, K. Arima, H. Tabunoki, J. Satoh, TDP-43 dimerizes in human cells in culture, Cell. Mol. Neurobiol. 30 (2010) 641–652.
[31] Y. Shamoo, N. Abdul-Manan, K.R. Williams, Multiple RNA binding domains (RBDs) just don't add up, Nucleic Acids Res. 23 (1995) 725–728.
[32] V. Swarup, D. Phaneuf, N. Dupre, S. Petri, M. Strong, J. Kriz, J.P. Julien, Deregulation of TDP-43 in amyotrophic lateral sclerosis triggers nuclear factor kappaB-mediated pathogenic pathways, J. Exp. Med. 208 (2011) 2429–2447.
[33] S.D. Auweter, F.C. Oberstrass, F.H.-T. Allain, Sequence-specific binding of single-stranded RNA: is there a code for recognition?, Nucleic Acids Res 34 (2006) 4943–4959.